

values of  $u_{ij+1}$  and  $l_{ij+1}$  were kept at 3.8 Å, and those for  $d_{ij+2}$ ,  $d_{ij+3}$ , and  $d_{ij+4}$  were adjusted by the triangle inequality. In general, the values of  $u_{ij}$  and  $l_{ij}$  for small  $|i-j|$  have little effect in constraining the conformation of the whole protein.

- (40) A cutoff distance of 10 Å for both the "contact" and "noncontact" distances means that  $u_{ij} = 10$  Å and  $l_{ij} = 5$  Å if  $d_{ij}^* < 10$  Å, and  $u_{ij} = 40$  Å and  $l_{ij} = 10$  Å if  $d_{ij}^* > 10$  Å. The triangle inequalities (6) are then applied to every set of three points to modify all of the  $u_{ij}$ 's and  $l_{ij}$ 's, except  $u_{i,i+1}$  and  $l_{i,i+1}$ , which are then used to calculate  $H$ .

- (41) Sternberg, M. J. E.; Thornton, J. M. *J. Mol. Biol.* **1976**, *105*, 367. *Ibid.* **1977**, *110*, 269, 285.  
 (42) Richardson, J. S. *Nature (London)* **1977**, *268*, 495.  
 (43) Chothia, C.; Levitt, M.; Richardson, D. *Proc. Natl. Acad. Sci. U.S.A.* **1977**, *74*, 4130.  
 (44) Richmond, T. J.; Richards, F. M. *J. Mol. Biol.* **1978**, *119*, 537.  
 (45) Cohen, F. E.; Sternberg, M. J. E.; Taylor, W. R. *Nature (London)* **1980**, *285*, 378.  
 (46) Shannon, C. E. *Bell Syst. Tech. J.* **1948**, *27*, 379, 623.

## NMR and ESR Study of the Conformations and Dynamical Properties of Poly(L-lysine) in Aqueous Solutions

B. Perly,\* Y. Chevalier, and C. Chachaty

Département de Physico-Chimie, Centre d'Etudes Nucléaires de Saclay, 91191 Gif-sur-Yvette Cedex, France. Received August 13, 1980

**ABSTRACT:** The conformations and dynamical behavior of poly(L-lysine) (PLL) in aqueous solutions have been investigated by  $^1\text{H}$  and  $^{13}\text{C}$  NMR as well as by ESR on the end-chain spin-labeled polymer. The ESR allowed the motion of the macromolecular chain to be studied up to pH 13, showing that the random coil  $\rightarrow \alpha$ -helix transition at pH 11 gives rise to a twofold increase in the correlation time, with evidence of an anisotropic reorientation. In the random coil state at pH 7, where the segmental motion of the backbone is quasi-isotropic, the correlation time given by ESR is compared to that obtained by the relaxation of the methyl protons of the reduced Tempo radical residue and of the  $\alpha$  carbons. The different methods yield an activation energy of 6.5 kcal mol $^{-1}$  for this motion whereas the frequency dependence of the  $C_\alpha$  relaxation may be interpreted by a Cole-Cole distribution of correlation times with a width parameter  $\gamma = 0.7$ . The rotational isomerism and temperature dependences of interconversion rates of the aminobutyl side chains have been analyzed from the proton vicinal couplings and the  $^{13}\text{C}$  and  $^1\text{H}$  relaxation at different frequencies, assuming that the methylene groups undergo 120° jumps among three sites, two of them being equiprobable. These two kinds of information concur to show that the PLL side chains are less flexible than a hydrocarbon chain of same length, possibly because of the hydration of the  $\text{NH}_3^+$  terminal group.

### Introduction

Among homopolypeptides, which may be considered as the simplest models for natural proteins, poly(L-lysine) (PLL) has been subjected to a great deal of study on its conformational properties as well as its biological activity.<sup>1</sup>

In aqueous solution, poly(L-lysine) is known to exist in several forms, namely, random coil,  $\alpha$  helix, and  $\beta$  sheets, depending upon pH and temperature. The random coil  $\rightarrow \alpha$ -helix transition which occurs around pH 11 has been investigated by several NMR techniques,<sup>2</sup> in particular by  $^1\text{H}$  chemical shifts<sup>3</sup> and  $^{13}\text{C}$  longitudinal relaxation,<sup>4</sup> the latter method giving semiquantitative information on the segmental mobility of the polymer. More recently, poly(L-lysine) in the  $\alpha$ -helix form was taken as a model in a theoretical study of the motion of an alkyl chain attached to a rigid rod undergoing an anisotropic overall motion.<sup>5</sup>

The present work deals mainly with the dynamical behavior and the conformational properties of poly(L-lysine) in the random coil state by  $^1\text{H}$  and  $^{13}\text{C}$  NMR and relaxation, i.e., below pH (or pD) 10, where well-resolved spectra may be obtained. Special attention has been paid to the relationship between the nuclear relaxation data, the proton vicinal coupling constants, and the rotational isomerism about each of the C-C bonds of the aminobutyl side chains.

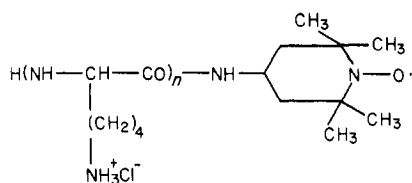
As a complement to the NMR studies, ESR experiments on the spin-labeled polymer provide a straightforward determination of the segmental motion of the main chain in both random coil and  $\alpha$ -helix structures. A direct comparison with proton relaxation data has been provided

by a diamagnetic analogue of the spin label.

### Experimental Section

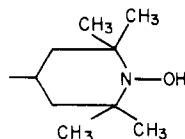
**Materials.** Poly(L-lysine) has been prepared by polymerization of L-lysine, the  $\epsilon$ -amino group being protected by trifluoroacetylation. This procedure was preferred to the original one of Fasman et al.<sup>6</sup> because the group must be removable under mild conditions, particularly in the case of a spin-labeled polymer.  $N^\epsilon$ -(Trifluoroacetyl)-L-lysine was prepared from L-lysine and *S*-ethyl trifluorothioacetate according to the procedure of Calvin et al.<sup>7</sup> Conversion to  $N^\epsilon$ -(trifluoroacetyl)-L-lysine *N*-carboxyanhydride ( $N^\epsilon$ -TFA-L-Lys-NCA) was performed by treatment with 4 M phosgene solution in tetrahydrofuran.<sup>8</sup> Prior to use NCA was recrystallized from ethyl acetate/petroleum ether.  $N^\epsilon$ -TFA-L-Lys-NCA [2.68 g ( $10^{-2}$  mol)] was dissolved in 25 mL of anhydrous dimethylformamide. After addition of 10 mg ( $10^{-4}$  mol) of *n*-hexylamine (monomer/initiator ratio = 100), polymerization was allowed to proceed at room temperature under continuous stirring for 2 days. Precipitation in 100 mL of water yielded 2.0 g (89%) of poly[ $N^\epsilon$ -(trifluoroacetyl)-L-lysine]. The trifluoroacetyl group was removed by dissolving 0.34 g of poly[ $N^\epsilon$ -(trifluoroacetyl)-L-lysine] into 7.5 mL of a 1 M piperidine solution in methanol. After 2 h, 5 mL of 1 M aqueous piperidine was added dropwise under stirring to the latter solution. After 2 days, the resulting clear solution was dialyzed for 5 days against circulating distilled water at 5 °C and then against a  $10^{-3}$  M HCl aqueous solution for 2 days. Finally the solution was freeze-dried, yielding 205 mg (80%) of poly(L-lysine) hydrochloride as a white fibrous material.

The spin-labeled poly(L-lysine) (Tempo-PLL) was synthesized following the same procedure as reported above, replacing *n*-hexylamine by 17 mg ( $10^{-4}$  mol) of 4-amino-2,2,6,6-tetramethylpiperidinyl-*N*-oxy (Tempo) as initiator. The diamagnetic



Tempo-PLL

analogue of Tempo-PLL was obtained by adding to a 0.1 M solution of PLL 2 equiv of freshly prepared sodium ascorbate solution. The reduction of the Tempo group to



occurred almost immediately, as checked by ESR. The excess reagent was removed by dialysis for 5 days against distilled water at 5 °C.

The molecular weights of the polymers were determined by measurement of the intrinsic viscosity of 1 M NaCl solutions of PLL at pH 3,<sup>6</sup> yielding  $125 < \overline{DP} < 145$ , according to the samples. The ESR measurements of radical concentration in the spin-labeled poly[N<sup>ε</sup>-(trifluoroacetyl)-L-lysine] yielded a  $\overline{DP}$  of 146. After removal of the TFA groups we obtained a  $\overline{DP}$  of 138, showing that there is virtually neither chain degradation nor deletion of radical end groups in the course of piperidine treatments. Likewise, the integrated intensity of the methyl protons in the diamagnetic reduced forms of Tempo-PLL gives a  $\overline{DP}$  of 140. Since all these polymers were prepared under identical conditions ([monomer]/[initiator] = 100), we may assume that the average degree of polymerization of the PLL under study is 140, with a comparatively low polydispersity.<sup>9</sup>

**NMR and ESR Experiments.** For NMR experiments, a stock solution of PLL was prepared in D<sub>2</sub>O after treatment at pD 7.5 with Chelex 100 chelating resin to remove metallic impurities. The solution was then twice freeze-dried from 99.8% D<sub>2</sub>O at pD 7 (pH meter reading). Before use, PLL hydrochloride was dissolved in 99.95% or 99.8% D<sub>2</sub>O for <sup>1</sup>H and <sup>13</sup>C experiments, respectively. After pD adjustment the solution was flushed with dry nitrogen gas in the NMR tube to remove dissolved oxygen.

All NMR measurements have been performed in the Fourier transform mode by means of Bruker WH90 [ $\nu(^{13}\text{C}) = 22.6$  MHz], Varian XL-100 [ $\nu(^1\text{H}) = 100$  MHz], and CAMECA TSN-250 [ $\nu(^{13}\text{C}) = 62.86$  MHz,  $\nu(^1\text{H}) = 250$  MHz] spectrometers.

The longitudinal relaxation times,  $T_1$ , were obtained by the inversion-recovery method ( $180^\circ - \tau - 90^\circ$  sequences), the interval between each sequence being at least equal to  $5T_1$ . The nuclear Overhauser enhancements (NOE) were obtained by the inverse gated decoupling method, with long-duration accumulations to ensure a signal-to-noise ratio not less than 50 for the spectra recorded without enhancement. The actual accuracy of the NOE measurements is  $\pm 5\%$ . In all experiments, the probe temperature was regulated within  $\pm 1$  °C.

The ESR experiments on Tempo-PLL were performed with a Varian E-109 X-band spectrometer, the magnetic field being calibrated by means of a Varian F-8 magnetometer.

## Results and Discussion

**Motion of the Macromolecular Backbone and the Random Coil  $\rightarrow \alpha$ -Helix Transition.** The conformational changes of poly(amino acids) in solution, in particular PLL and PLGA, have been investigated by a variety of techniques,<sup>1</sup> including NMR.<sup>2</sup> The random coil  $\rightarrow \alpha$ -helix transition is clearly evidenced by a sharp variation of <sup>1</sup>H chemical shifts.<sup>3</sup> Similar measurements performed on the polymer under study ( $\overline{DP} = 140$ ) gave us a transition midpoint at pD 10.8. This transition has been also studied by <sup>13</sup>C  $T_1$  and chemical shift determinations as functions of pH,<sup>4</sup> but the broadening of the lines

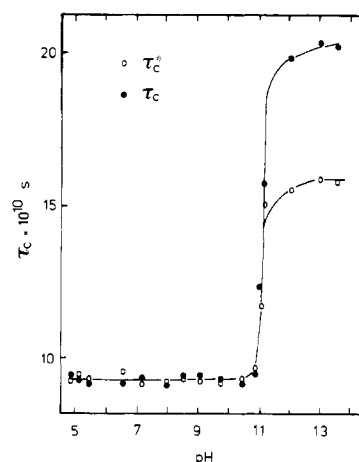


**Figure 1.** pH dependence of the reorientation correlation time of the nitroxide terminal group in 0.1 M Tempo-PLL measured by ESR at 5 °C.

precluded experiments on the  $\alpha$ -helix form above pD 11.

For the measurement of the change in the segmental mobility of the main chain of PLL at the random coil  $\rightarrow \alpha$ -helix transition, it seemed to us that it was preferable to perform ESR experiments on Tempo-PLL up to pD 13 on dilute ( $< 0.1$  M) H<sub>2</sub>O solutions. Above pH 11, the precipitation of PLL in the  $\beta$ -sheet form was avoided by cooling at 5 °C.<sup>10</sup> Under most of our experimental conditions, the nitroxide radical at the chain end gives rise to three equally spaced ESR lines (absorption first derivative), the  $\Delta\nu_{ms}$  peak-to-peak width of which depends upon the relevant nitrogen quantum number  $m_N = 0, \pm 1$ . From  $\Delta\nu_{ms}$ , the reorientation correlation time  $\tau_c$  may be obtained by the relation<sup>11</sup>

$$\pi\sqrt{3}\Delta\nu_{ms} = T_2^{-1}(m_N) \simeq [3b^2/20 + \frac{1}{45}(\Delta\gamma B_0)^2 + (b^2/8)m_N^2 - \frac{1}{15}b\Delta\gamma B_0 m_N]\tau_c + X \quad (1)$$

with

$$b = (4\pi/3)[A_{zz}^N - \frac{1}{2}(A_{xx}^N + A_{yy}^N)] = 2\pi(A_{zz}^N - A_{iso}^N) \quad (2)$$

$$\Delta\gamma = -(\beta/\hbar)[g_{zz} - \frac{1}{2}(g_{xx} + g_{yy})] = (3\beta/2\hbar)(g_{zz} - g_{iso}) \quad (3)$$

In eq 1,  $B_0$ , the static magnetic field, is 3250 G, and  $b$  and  $\Delta\gamma$  represent the anisotropy of the  $\mathbf{A}$  and  $\mathbf{g}$  tensors, respectively.  $A_{iso}^N = 47$  MHz,  $A_{zz}^N = 99.9$  MHz,  $g_{iso} = 2.0055$ , and  $g_{zz} = 2.0022$  were readily obtained from the ESR spectrum of Tempo-PLL in aqueous solution at room temperature or frozen at 100 K.  $X$  is the contribution to the electron transverse relaxation rate  $T_2^{-1}$ , independent of  $\tau_c$ .

$I_0$ ,  $I_+$ , and  $I_-$  being the amplitudes of the  $m_N = 0, +1, -1$  ESR lines (absorption first derivatives), it is shown<sup>12</sup> that two correlation times may be obtained from the coefficients of  $m_N$  and  $m_N^2$  in eq 1:

$$\tau_c = \frac{15T_2^{-1}(0)}{8b\Delta\gamma B_0} \left[ \left( \frac{I_0}{I_-} \right)^{1/2} - \left( \frac{I_0}{I_+} \right)^{1/2} \right] \quad (4)$$

$$\tau_c^* = \frac{4T_2^{-1}(0)}{b^2} \left[ \left( \frac{I_0}{I_+} \right)^{1/2} + \left( \frac{I_0}{I_-} \right)^{1/2} - 2 \right] \quad (5)$$

The difference between  $\tau_c$  and  $\tau_c^*$  is a criterion for the anisotropy of the motion of the nitroxide group.<sup>13</sup>

Figure 1 gives the pH dependence of the  $\tau_c$  and  $\tau_c^*$  correlation times, which show a steep increase at the random coil  $\rightarrow \alpha$ -helix transition, occurring at pH 11 in

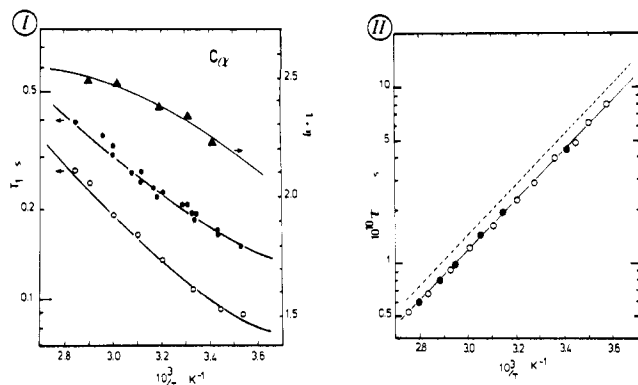


**Figure 2.** (I)  $^{13}\text{C}$  NOE at 22.63 MHz ( $\blacktriangle$ ) and  $T_1$  relaxation times at 62.86 ( $\bullet$ ) and 22.63 MHz ( $\circ$ ). The solid lines have been calculated for the Cole-Cole distribution of correlation times  $\tau_R$  ( $\gamma = 0.7$ ), taking  $\bar{\tau}_R = 7.57 \times 10^{-15} \exp(6500 \text{ cal mol}^{-1}/RT)$  s. (II) Temperature dependences of correlation times  $\tau_R$  (dotted line) and  $\tau_c$ , the latter being obtained from ESR line widths ( $\circ$ ) and methyl proton relaxation of the reduced Tempo group ( $\bullet$ ). These diagrams are given for PLL in the random coil state at pH 7.

$\text{H}_2\text{O}$ , instead of pD 10.8 in  $\text{D}_2\text{O}$  (meter reading; see above), so that we assume as previously<sup>14</sup> that pD  $\approx$  pH. At room temperature below pH 11, in the random coil form, isotropic motion is observed, with  $\tau_c = \tau_c^* \approx 5 \times 10^{-11}$  s, whereas a marked anisotropy effect appears above pH 11, with  $\tau_c \approx 1.5 \times 10^{-9}$  and  $\tau_c^* \approx 2 \times 10^{-9}$  s. The reorientation correlation times in the  $\alpha$ -helix form are significantly shorter than expected for a rigid-rod form, the diffusion coefficients of which are<sup>15</sup>

$$D_{\perp} = \frac{3kTM_0^3}{2\pi\eta d^3M^3} \left[ 2 \ln \left( \left( \frac{2}{3} \right)^{1/2} \frac{Md}{M_0R} \right) - 1 \right] \quad (6)$$

$$D_{\parallel} = \frac{kTM_0}{4\pi\eta R^2Md} \left[ 1 - \frac{6M_0^2R^2}{M^2d^2} \ln \left( \left( \frac{2}{3} \right)^{1/2} \frac{Md}{M_0R} \right) \right] - D_{\perp} \quad (7)$$

$M_0$  and  $M$  are the molecular weights of the monomer residue and of the polymer, respectively;  $M/M_0 = 140$ ,  $d$ , the increment of the helix length per monomer residue, is 1.5 Å,  $R$ , the helix radius, is 7.5 Å, and  $\eta$ , the viscosity of water at 278 K, is 1.512 cP. From eq 6 and 7,  $D_{\perp} = 6.8 \times 10^5$  and  $D_{\parallel} = 1.7 \times 10^7$  rad s<sup>-1</sup>. Although  $D_{\parallel}$  and  $D_{\perp}$  cannot be obtained by ESR in the present case since the orientation of the N–O group with respect to the macromolecule backbone is not known, it is seen that  $\tau_c$  and  $\tau_c^*$  are much smaller indeed than  $2.7 \times 10^{-8}$  s, the value of  $\langle \tau_c \rangle = 1/2(D_{\parallel} + 2D_{\perp})^{-1}$ .

The ESR measurements on PLL in the random coil state indicate a quasi-isotropic motion of the chain end, with  $\tau_c = \tau_c^*$  (Figure 1). This correlation time may also be calculated from the longitudinal relaxation of methyl protons in Tempo-PLL after reduction by ascorbic acid. Since the correlation time for the axial reorientation of  $\text{CH}_3$  is most likely of the order of  $10^{-11}$  s or less, it may be shown<sup>16,17</sup> that the relaxation rate of a proton pair of this group is

$$\frac{1}{T_1} \approx \frac{3\gamma_H^4\hbar^2}{80\tau^6} (3 \cos^2 \Delta - 1)^2 \left[ \frac{2\tau_R}{1 + \omega_H^2\tau_R^2} + \frac{8\tau_R}{1 + 4\omega_H^2\tau_R^2} \right] \quad (8)$$

where  $\tau_R$  is the correlation time for the segmental motion at the chain ends and  $\Delta$ , the angle between a H–H vector

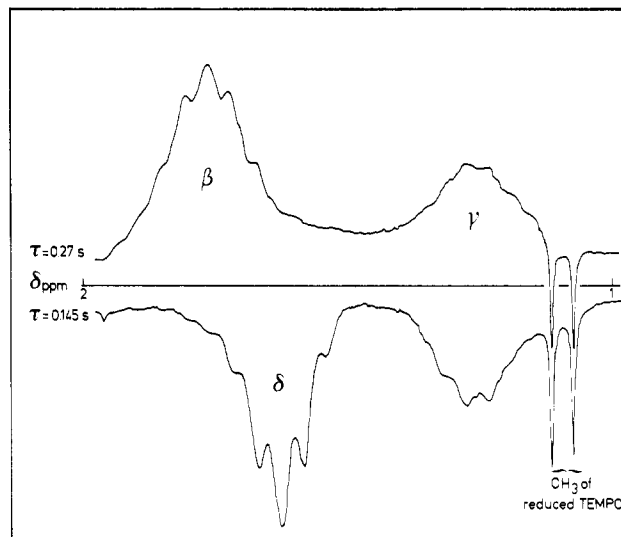


**Figure 3.** Separation by inversion-recovery of the  $\text{H}_\beta$  and  $\text{H}_\gamma$  resonances in the 250-MHz  $^1\text{H}$  NMR spectrum of PLL at 350 K and pH 7.

and the rotation axis of  $\text{CH}_3$ , is  $90^\circ$ . Figure 2-II shows that there is an excellent agreement between  $\tau_c$  and  $\tau_R$  which are close to the mean correlation time  $\bar{\tau}_R$  determined by  $^{13}\text{C}$  relaxation for the segmental motions of the whole chains. The longitudinal relaxation of  $\alpha$  carbons is given by<sup>18</sup>

$$1/T_1 = 1/10 \gamma_H^2 \gamma_C^2 \hbar^2 r_{\text{CH}}^{-6} [J_0(\omega_H - \omega_C) + 3J_1(\omega_C) + 6J_2(\omega_H + \omega_C)] \quad (9)$$

The nuclear Overhauser enhancement of carbons observed under proton noise decoupling is<sup>18</sup>

$$\text{NOE} = 1 + \frac{\gamma_H}{\gamma_C} \frac{6J_2(\omega_H + \omega_C) - J_0(\omega_H - \omega_C)}{J_0(\omega_H - \omega_C) + 3J_1(\omega_C) + 6J_2(\omega_H + \omega_C)} \quad (10)$$

In eq 9 and 10 the  $J(\omega)$  are the spectral densities expressed as a function of proton and carbon Larmor angular frequencies. The  $^{13}\text{C}_\alpha$  longitudinal relaxation and NOE have been measured at different temperatures at pH 7, where PLL is entirely in the random coil state.<sup>19</sup> The comparison of the data obtained at 22.6 and 62.86 MHz (Figure 2-I) suggests the existence of a distribution of correlation times represented by a function  $G(\tau_R)$ , the spectral densities being expressed as

$$J(\omega) = \int_0^\infty \frac{\tau_R G(\tau_R)}{1 + \omega^2 \tau_R^2} d\tau_R \quad (11)$$

We assume, as in previous works<sup>14,20,21</sup> a Cole-Cole distribution.<sup>22</sup> Therefore, the spectral density is given by<sup>23</sup>

$$J(\omega) = \frac{1}{2\omega} \frac{\cos[(1 - \gamma)(\pi/2)]}{\cosh(\gamma \ln \omega \bar{\tau}_R) \sin[(1 - \gamma)(\pi/2)]} \quad (12)$$

where  $\gamma$  is a parameter characterizing the distribution width and  $\bar{\tau}_R$  is the central value of this distribution.

The NOE and  $T_1$  relaxation time as a function of  $1/T$  at the two spectrometer frequencies are consistent with  $\gamma = 0.7$  and  $\bar{\tau}_R = 7.56 \times 10^{-15} \exp(6500/RT)$ . The same activation energy of 6.5 kcal mol<sup>-1</sup> is found in ESR,  $^1\text{H}$ , and  $^{13}\text{C}$  relaxation experiments (Figure 2), the correlation time at the chain end given by the two former methods being shorter by only  $\sim 12\%$  than  $\bar{\tau}_R$ . The motional freedom at chain ends is therefore slightly higher than the average segmental mobility of the macromolecular backbone. Here again, the relevant correlation time  $\bar{\tau}_R$  is much smaller than

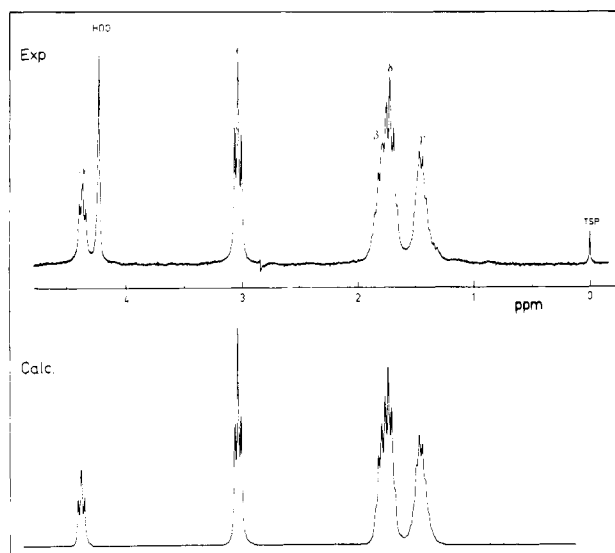


Figure 4. Proton NMR spectrum at 250 MHz, pH = 7, and  $T = 350$  K. The lower trace has been simulated with the parameters of Table I.

Table I  
Proton Chemical Shifts and Coupling Constants of PLL at 350 K and pD 7 Used in the Simulation of the NMR Spectrum of PLL (Figure 4)

Chemical Shifts <sup>a</sup>						
H <sub>α</sub>	H <sub>β<sub>1</sub></sub>	H <sub>β<sub>2</sub></sub>	H <sub>γ<sub>1</sub></sub>	H <sub>γ<sub>2</sub></sub>	H <sub>δ<sub>1,2</sub></sub>	H <sub>ε<sub>1,2</sub></sub>
4.30	1.756	1.827	1.420	1.394	1.673	2.989
Coupling Constants <sup>b</sup>						
J <sub>αβ<sub>1</sub></sub> = 6.06		J <sub>αβ<sub>2</sub></sub> = 7.76				
J <sub>β<sub>1</sub>γ</sub> = 6.50		J <sub>β<sub>2</sub>γ</sub> = 7.70				
J <sub>γδ</sub> = 7.07		J <sub>δε</sub> = 7.56				
J <sub>β<sub>1</sub>β<sub>2</sub></sub> = J <sub>γ<sub>1</sub>γ<sub>2</sub></sub> = J <sub>δ<sub>1</sub>δ<sub>2</sub></sub> = J <sub>ε<sub>1</sub>ε<sub>2</sub></sub> = -14						

<sup>a</sup> In ppm from sodium 3-(trimethylsilyl)propionate-2,2,3,3- $d_4$ . <sup>b</sup> In Hz.

expected from the overall dimensions of the macromolecule, the gyration radius of which is

$$\langle R_G^2 \rangle = Kl^2(DP) \quad (13)$$

For  $\overline{DP} = 140$ ,  $l = 3.77$  Å (length of the monomer unit), and  $K = 1.3^{24}$  one finds  $\langle R_G^2 \rangle^{1/2} = 50.8$  Å. For a rigid spherical structure at 20 °C in aqueous solution, one should have indeed  $\tau_R = 1.3 \times 10^{-7}$  s instead of the observed value of  $5 \times 10^{-10}$  s.

**Conformations and Segmental Motions of Side Chains at pD 7.** The rotamers of the side chain and their interconversion rates have been determined by  $^1H$  and  $^{13}C$  NMR relaxation. The 250-MHz  $^1H$  NMR spectrum of PLL at 350 K and pD 7 is shown in Figure 4. Under our experimental conditions, the  $H_\beta$  and  $H_\delta$  resonances are partially superimposed, giving a complex pattern, the two components of which have been separated by inversion-recovery (Figure 3). For time intervals of 0.145 and 0.27 s between the 180° and 90° pulses, the  $\beta$  and  $\delta$  resonances are successively canceled, allowing the other one to be selectively observed. The  $^1H$  NMR spectrum of PLL has been simulated by means of the SIMEQ program from Varian, using the parameters given in Table I (Figure 4).

The proton vicinal coupling constants have been interpreted in terms of rotamer populations about the C-C bonds, taking  $^3J_t = 12.4$  Hz and  $^3J_g = 3.25$  Hz as given by Kopple's modification of the Karplus relation<sup>25</sup>

$$^3J_{HH} = 11.0 \cos^2 \theta - 1.4 \cos \theta + 1.6 \sin^2 \theta \quad (14)$$

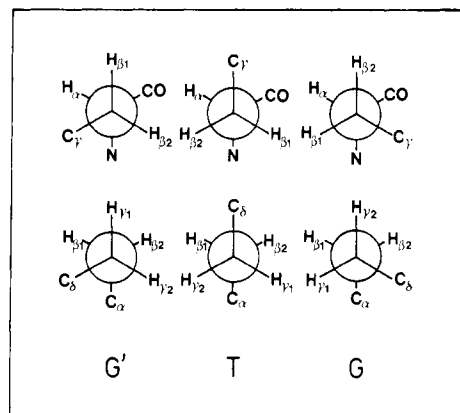


Figure 5. Classical rotamers about the C-C bonds of the side chains.

where  $\theta$  is the HCCH dihedral angle.

The populations of the classical T (trans), G, and G' (gauche) rotamers about the C-C bonds of the side chains (Figure 5) are related by

$$P_T + P_G + P_{G'} = 1 \quad (15)$$

The couplings between the  $\alpha$  and  $\beta$  protons yield

$$P_T = \frac{J_{\alpha\beta_1} - J_g}{J_t - J_g} \quad P_{G'} = \frac{J_{\alpha\beta_2} - J_g}{J_t - J_g} \quad (16a)$$

and therefore

$$P_G = \frac{J_t + J_g - (J_{\alpha\beta_1} + J_{\alpha\beta_2})}{J_t - J_g} \quad (16b)$$

For the  $\beta$  and  $\gamma$  protons, we have likewise

$$P_T = \frac{J_{\beta_1\gamma_1} - J_g}{J_t - J_g} = \frac{J_{\beta_2\gamma_1} - J_g}{J_t - J_g} \quad (17a)$$

$$P_{G'} = \frac{J_{\beta_1\gamma_2} - J_g}{J_t - J_g} \quad (17b)$$

$$P_G = \frac{J_{\beta_2\gamma_1} - J_g}{J_t - J_g} \quad (17c)$$

These populations may be also expressed as functions of the mean coupling constants  $\bar{J}_{\beta_1\gamma} = 1/2(J_{\beta_1\gamma_1} + J_{\beta_1\gamma_2})$  and  $\bar{J}_{\beta_2\gamma} = 1/2(J_{\beta_2\gamma_1} + J_{\beta_2\gamma_2})$  obtained from the simulation of the  $^1H$  NMR spectrum of PLL (Table I)

$$P_G = 1 - \frac{2(\bar{J}_{\beta_1\gamma} - J_g)}{J_t - J_g} \quad (18a)$$

$$P_{G'} = 1 - \frac{2(\bar{J}_{\beta_2\gamma} - J_g)}{J_t - J_g} \quad (18b)$$

$$P_T = \frac{2(\bar{J}_{\beta_1\gamma} + \bar{J}_{\beta_2\gamma} - 2J_g)}{J_t - J_g} - 1 = \frac{4(\bar{J}_{\beta\gamma} - J_g)}{J_t - J_g} - 1 \quad (18c)$$

where  $\bar{J}_{\beta\gamma} = 1/2(\bar{J}_{\beta_1\gamma} + \bar{J}_{\beta_2\gamma})$ .

The  $\bar{J}_{\beta_1\gamma_1}$  and  $\bar{J}_{\beta_2\gamma_2}$  which are not directly available from the analysis of the NMR spectrum of PLL, may be obtained by combining eq 17 and 18

$$\bar{J}_{\beta_1\gamma_1} = 3\bar{J}_{av} - 2\bar{J}_{\beta_2\gamma} \quad (19a)$$

$$\bar{J}_{\beta_2\gamma_2} = 3\bar{J}_{av} - 2\bar{J}_{\beta_1\gamma} \quad (19b)$$

$$\bar{J}_{\beta_1\gamma_2} = \bar{J}_{\beta_2\gamma_1} = 4\bar{J}_{\beta\gamma} - 3\bar{J}_{av} \quad (19c)$$

where  $\bar{J}_{av} = (J_t + 2J_g)/3$ .

Table II  
Rotamer Populations of PLL Side Chains Obtained from  
Vicinal Coupling Constants

population			
$C_\alpha-C_\beta$	$P_T^a = 0.32$	$P_{G'}^a = 0.49$	$P_G = 0.19$
$C_\beta-C_\gamma$	$P_T = 0.68$	$P_{G'} = 0.03$	$P_G = 0.29$
$C_\gamma-C_\delta$	$P_T = 0.67$	$P_G + P_{G'} = 0.33$	
$C_\delta-C_\epsilon$	$P_T = 0.88$	$P_G + P_{G'} = 0.12$	

<sup>a</sup> Tentative assignment.

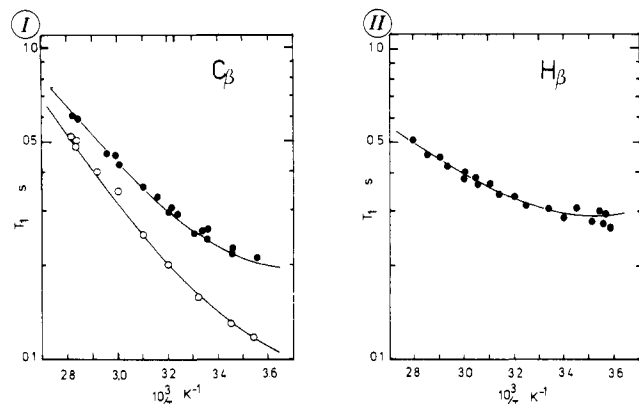


Figure 6. (I)  $\beta$ -carbon  $2T_1$  relaxation times at 22.63 (○) and 62.86 MHz (●). (II)  $\beta$ -proton  $T_1$  relaxation times at 250 MHz. The solid lines have been computed with parameters of Table III. In this figure and the following ones the  $^{13}\text{C}$  relaxation times are given as twice the actual value since the methylene carbons are relaxed by the two adjacent protons.

For the  $(\text{CH}_2)_\gamma(\text{CH}_2)_\delta(\text{CH}_2)_\epsilon$  residue, where only  $J_{\gamma\delta}$  and  $J_{\delta\epsilon}$  are available, the population of the trans rotamer is given by an expression similar to (18c).

It is seen from eq 15–19 that since the measured vicinal coupling constants cannot be generally assigned to given proton pairs, the determination of the population of the three rotamers is achieved only for the  $(\text{CH}_2)_\beta(\text{CH}_2)_\gamma$  fragment. In the case of the  $(\text{CH})_\alpha(\text{CH}_2)_\beta$  residue, however, the G' rotamer is likely the most populated,<sup>26</sup> as confirmed by experiments in progress on the paramagnetic relaxation induced by  $\text{Gd}^{3+}$  in  $\alpha$ -amino acids and oligopeptides. Among the rotamers about the  $C_\gamma-C_\delta$  and  $C_\delta-C_\epsilon$  bonds, only the population of the trans ones can be determined unambiguously. The populations of different rotamers of the PLL side chains are given in Table II.

The proton and  $^{13}\text{C}$  relaxation times in side chains have been interpreted by assuming that rotational jumps about C–C bonds occur between three sites, two of them, denoted as 2 and 3, being equiprobable. The motion about the these bonds is specified by the jump rates  $W_1$  (site 1  $\rightarrow$  site 2 or 3),  $W_2$  (site 2 or 3  $\rightarrow$  site 1),  $W_3$  (site 2  $\rightleftharpoons$  site 3).<sup>5,20,27</sup> In these calculations, it is assumed that site 1 corresponds to the trans conformer of the C–C–C–C fragments.

The populations of the sites are given by

$$P_1 = 1/(2\nu + 1) \quad P_2 = P_3 = \nu/(2\nu + 1) \quad (20)$$

with  $\nu = W_1/W_2$ ;  $W_3$  has only an influence on the effective correlation times governing the relaxation of side-chain nuclei. The expressions of the spectral densities intervening in eq 9 and 10, which depend also on the distribution of correlation times  $\tau_R$ , may be found in ref 20.

As pointed out previously,<sup>21</sup> the determination of  $W_1$ ,  $W_2$ , and  $W_3$  has to be done by relaxation measurements at different spectrometer frequencies and preferably on different nuclei. We have therefore determined for each of the methylene groups the  $^{13}\text{C}$  relaxation at 22.6 and

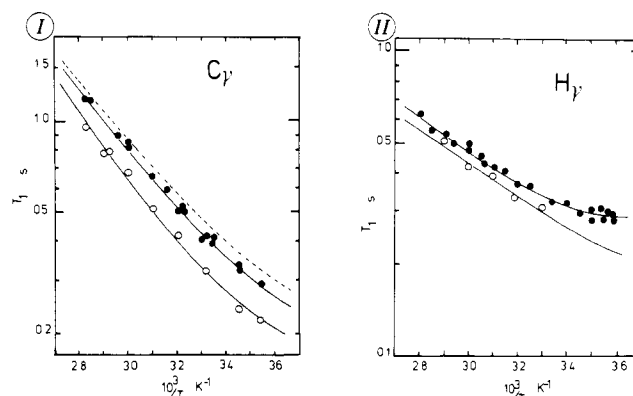


Figure 7. (I)  $2T_1$  of  $^{13}\text{C}_\gamma$  at 22.63 (○) and 62.86 MHz (●). (II) Proton  $T_1$  relaxation times at 100 (○) and 250 MHz (●). The solid lines are computed with the parameters of Table III. In panel I the dotted line corresponds to  $W_1/W_2 = 0.232$  (parameter obtained from  $^3J_{\text{HH}}$ ),  $W_0 = 7 \times 10^{11} \text{ s}^{-1}$ , and  $\Delta H = 3.7 \text{ kcal/mol}$  for a spectrometer frequency of 62.86 MHz.

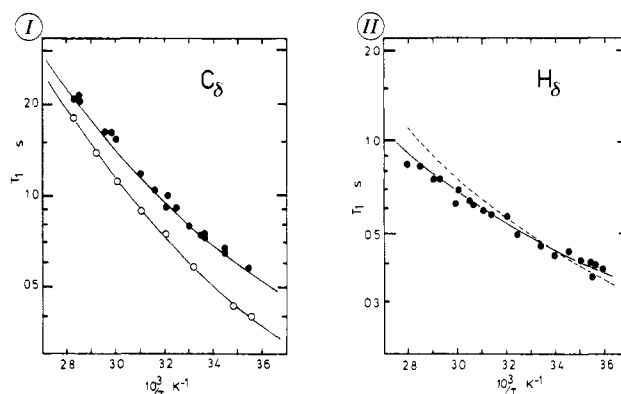


Figure 8. (I)  $2T_1$  of  $^{13}\text{C}_\delta$  at 22.63 (○) and 62.86 MHz (●). The solid lines are computed with the parameters corresponding to models I and II of Table III. (II)  $\delta$ -proton  $T_1$  relaxation times at 250 MHz (●). Solid line, model I; dotted line, model II.

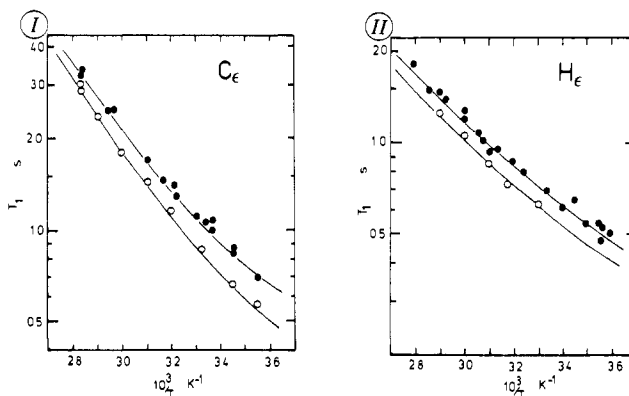


Figure 9. (I)  $2T_1$  relaxation time of  $C_\epsilon$  at 22.63 (○) and 62.86 MHz (●). (II)  $T_1$  of  $H_\epsilon$  at 100 (○) and 250 MHz (●). The solid lines are calculated with the parameters of Table III for models I and II.

62.86 MHz as well as the  $^1\text{H}$  relaxation at 250 MHz and in some cases at 100 MHz also (Figure 6–9). The methylene protons being separated by only 1.78 Å (for C–H: C–H = 1.09 Å, H–C–H = 109.5°), their mutual dipolar interaction is the main relaxation mechanism. The longitudinal relaxation of these protons is nearly exponential; i.e., there is no significant deviation of the semilogarithmic plot of  $(M_0 - M_z)/2M_0$  from the tangent at  $t = 0$ . The contribution of vicinal protons to the relaxation of methylene protons, which is appreciably reduced by the rotation

Table III  
Rotamer Populations and Kinetic Parameters of PLL Side Chains from  $^1\text{H}$  and  $^{13}\text{C}$  Relaxation Measurements

$P_1$					$P_2 = P_3$			
$C_\alpha-C_\beta$		0.2				0.40		
$C_\beta-C_\gamma$		0.5				0.25		
$C_\gamma-C_\delta$	I {0.67 0.88		II {0.2 0.2		I {0.165 0.06		II {0.40 0.40	
$C_\delta-C_\epsilon$								
	$(W_1)_0, \text{ s}^{-1}$	$W_1(300 \text{ K}), \text{ s}^{-1}$	$W_1/W_2$	$\Delta H^{\ddagger}_{1,2}, \text{ kcal mol}^{-1}$	$(W_3)_0, \text{ s}^{-1}$	$W_3(300 \text{ K}), \text{ s}^{-1}$	$\Delta H^{\ddagger}_3, \text{ kcal mol}^{-1}$	$r^*_{\text{HH}}, \text{ \AA}$
$C_\alpha-C_\beta$	$2.5 \times 10^{15}$	$4.4 \times 10^7$	2	10.6	$5 \times 10^{12}$	$6 \times 10^9$	4.0	1.738
$C_\beta-C_\gamma$	$5.0 \times 10^{11}$	$1.4 \times 10^9$	0.5	3.5	<i>a</i>	<i>a</i>	<i>a</i>	1.730
$C_\gamma-C_\delta$ (I)	$4.0 \times 10^{12}$	$2.9 \times 10^9$	0.25	4.3	<i>a</i>	<i>a</i>	<i>a</i>	1.710
$C_\gamma-C_\delta$ (II)	$1.2 \times 10^{14}$	$1.3 \times 10^6$	2	10.9	$2.5 \times 10^{14}$	$1.4 \times 10^{10}$	5.8	1.725
$C_\delta-C_\epsilon$ (I)	$1.0 \times 10^{14}$	$3.8 \times 10^9$	0.07	6.05	<i>a</i>	<i>a</i>	<i>a</i>	1.730
$C_\delta-C_\epsilon$ (II)	$1.2 \times 10^{13}$	$1.3 \times 10^5$	2	10.9	$7.0 \times 10^{15}$	$7.1 \times 10^9$	8.2	1.740

<sup>a</sup> The 2  $\rightleftharpoons$  3 transition rate is probably too slow compared with  $W_{1,2}$  to influence appreciably the nuclear relaxations.

about C-C bonds, was taken into account by introducing in our calculations an effective interproton distance slightly smaller than 1.78 Å. This correction has been discussed elsewhere.<sup>21</sup>

The temperature dependences of the  $^{13}\text{C}$  and  $^1\text{H}$   $T_1$  relaxation times have been simulated by assuming jump rates of the form

$$W_i = (W_i)_0 \exp(\Delta H_i/RT) \quad (21)$$

with  $i = 1-3$ ,  $\Delta H_i$  being the potential barriers between the sites (Figures 6-10). A good agreement between the experimental and computed relaxation rates is achieved by taking  $W_1/W_2$  constant in the investigated temperature range, 285 <  $T$  < 360 K. This approximation implies that the difference between the potential barriers  $\Delta H_1$  (1  $\rightarrow$  2, 3) and  $\Delta H_2$  (2, 3  $\rightarrow$  1) is comparatively small. In a hydrocarbon chain  $\Delta H_1 - \Delta H_2$  is indeed of the order of 0.5-0.6 kcal/mol.<sup>24</sup>

The populations  $P_{1,2,3}$  of the rotamers about C-C bonds of the side chain as well as the kinetic parameters for the rotational jumps, deduced from the relaxation data, are given in Table III. The calculations have been first carried out by introducing the values of  $W_1/W_2$  derived from the rotamer populations given by the Koppé's relationship (eq 14) and adjusting the jump rates  $W_1$ ,  $W_2$ , and  $W_3$  until the measured relaxation rates are fitted with an accuracy better than  $\pm 5\%$  at different temperatures (Figures 6-9). This process yields a satisfactory agreement for the relaxations of  $\text{C}_\beta$  and  $\text{H}_\beta, \text{H}_{\beta_2}$  (Figure 6). On the other hand, the value of 0.232 given by vicinal couplings for  $W_1/W_2$  is not convenient for the rotation about  $\text{C}_\beta\text{-C}_\gamma$ . A better agreement between the observed and computed relaxation rates of  $\text{C}_\gamma$ ,  $\text{H}_{\gamma_1}$ ,  $\text{H}_{\gamma_2}$  is achieved by taking  $W_1/W_2 = 0.5$ . This discrepancy results possibly from the large difference between the populations of the G and G' rotamers (Table II), which cannot be taken into account in the calculations of relaxation rates. On the other hand, the rotamer populations about  $\text{C}_\gamma\text{-C}_\delta$  and  $\text{C}_\delta\text{-C}_\epsilon$  derived from the vicinal coupling constants seem fairly consistent with the relaxations of the protons and carbons of the  $\delta$ - and  $\epsilon$ -methylene groups. It may be pointed out in particular that the conformation of the  $\text{C}_\gamma\text{-C}_\delta\text{-C}_\epsilon\text{-N}$  residue is nearly trans and that the effective  $\text{H}_\delta\text{-H}_\epsilon$  distance, which accounts for the proton relaxation, is actually that of the trans conformer of an alkyl chain.

Several attempts have been made to check whether significantly different sets of parameters can give reasonable fits of the temperature dependence of relaxation rates.

These attempts have not been successful for  $\beta$ - and  $\gamma$ -methylene groups. It appears, however, that two sets of parameters are convenient for  $(\text{CH}_2)_\delta$  and  $(\text{CH}_2)_\epsilon$ .

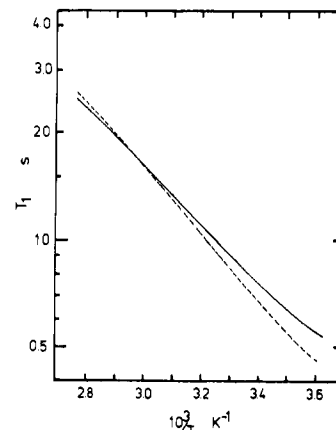


Figure 10.  $2T_1$  relaxation time of  $\text{C}_\beta$  calculated for a spectrometer frequency of 125 MHz ( $H_0 = 11.75 \text{ T}$ ) with the data of Table III. The solid and dotted lines correspond to models I and II, respectively.

One set, designated as I in Table III, derived in part from proton vicinal couplings as shown above, corresponds to an increasing population of the local trans conformer from the macromolecular backbone through the amino group of side chains. The other set (II) corresponds to a segmental motion occurring by fast exchange among the two equally populated conformers with  $P_T < P_G$ . The  $W_3$  jump rate becomes then effective in the relaxation process.

Figures 8 and 9 show that the agreement of models I and II with experiment is equivalent, the curves computed with the corresponding sets of parameters being superimposable except for  $\text{H}_\beta$ , where a small deviation between the observed and computed relaxation times is observed for model I as the temperature increases.

It should be expected that the discrimination between these two models can be performed by means of a spectrometer operating at a magnetic field of the order of 10 T, which is now available. Figure 10 shows that the difference between the relaxation times computed for  $\text{C}_\beta$  with  $W_1/W_2 \approx 0.250$  and 2 is not sufficient to make an unambiguous choice between the two models. Model II may be ruled out as incompatible with the  $^3J_{\text{HH}}$  couplings given in Table I, even if eq 14 is not strictly valid for the  $(\text{CH}_2)_\gamma(\text{CH}_2)_\delta(\text{CH}_2)_\epsilon$  fragment. This example shows that the analysis of vicinal proton couplings in terms of rotamer populations is sometimes essential in the interpretation of relaxation data.

## Conclusions

The magnetic resonance study of PLL in aqueous solution shows that the macromolecular backbone has a high

segmental mobility in the random coil state and remains flexible even in the  $\alpha$ -helix form, up to pD 13. The activation energy for the segmental motion of the main chain is of the order of 6 kcal/mol at pD 7, like poly(L-glutamic acid)<sup>14</sup> and poly[N<sup>5</sup>-(3-hydroxypropyl)-L-glutamine]<sup>21</sup> under similar conditions, confirming that in the random coil state the flexibility of polypeptides is nearly independent of the nature of side chains.<sup>28</sup>

The rotational isomerism and the jump rates of side-chain methylene group are quite different from those of a hydrocarbon chain attached to a macromolecule,<sup>29,30</sup> showing, in particular, for model I of segmental motion, which seems the most likely, a gradual decrease of the reorientational freedom from the main chain through the terminal group. In the present case the comparatively slow rotation of (CH<sub>2</sub>)<sub>4</sub> may be explained by the high hydration degree of the adjacent ND<sub>3</sub><sup>+</sup> group, which has been evidenced by NMR.<sup>31,32</sup>

**Acknowledgment.** We are greatly indebted to Dr. H. R. Wyssbrod for his helpful comments and suggestions concerning the interpretation of vicinal coupling constants in terms of rotamer populations.

## References and Notes

- (1) Fasman, G. D. "Poly-Amino Acids"; Marcel Dekker: New York, 1967, and references therein.
- (2) Bovey, F. A. *Macromol. Rev.* **1974**, *9*, 1.
- (3) Bradbury, E. M.; Crane-Robinson, C.; Goldman, H.; Rattle, H. W. E. *Biopolymers* **1968**, *6*, 851.
- (4) Saito, H.; Smith, I. C. P. *Arch. Biochem. Biophys.* **1973**, *158*, 154.
- (5) Wittebort, R. J.; Szabo, A. *J. Chem. Phys.* **1978**, *69*, 1722.
- (6) Fasman, G. D.; Idelson, M.; Blout, E. R. *J. Am. Chem. Soc.* **1961**, *83*, 709.
- (7) Schallenberg, E. M.; Calvin, M. *J. Am. Chem. Soc.* **1955**, *77*, 2779.
- (8) Fuller, W. D.; Verlander, M. S.; Goodman, M. *Biopolymers* **1976**, *15*, 1869.
- (9) Lundberg, R. D.; Doty, P. *J. Am. Chem. Soc.* **1957**, *79*, 3961.
- (10) Peggion, E.; Cosani, A.; Terbojevich, M.; Romanin-Jacur, L. *J. Chem. Soc., Chem. Commun.* **1974**, 314.
- (11) Kivelson, D. *J. Chem. Phys.* **1960**, *33*, 1094.
- (12) Stone, T. J.; Buckman, T.; Nordio, P. L.; McConnell, H. M. *Proc. Natl. Acad. Sci. U.S.A.* **1965**, *54*, 1010.
- (13) Goldman, S. A.; Bruno, G. V.; Polnaszek, C. F.; Freed, J. H. *J. Chem. Phys.* **1972**, *56*, 716.
- (14) Tsutsumi, A.; Perly, B.; Forchioni, A.; Chachaty, C. *Macromolecules* **1978**, *11*, 977.
- (15) Price, C.; Heatley, F.; Holton, T. J.; Harris, P. A. *Chem. Phys. Lett.* **1977**, *49*, 504.
- (16) Navon, G.; Lanir, A. *J. Magn. Reson.* **1972**, *8*, 144.
- (17) Marshall, A. G.; Schmidt, P. G.; Sykes, B. D. *Biochemistry* **1972**, *11*, 3875.
- (18) Doddrell, D.; Glushko, V.; Allerhand, A. *J. Chem. Phys.* **1972**, *56*, 3683.
- (19) Myer, Y. P. *Macromolecules* **1969**, *2*, 624.
- (20) Tsutsumi, A.; Chachaty, C. *Macromolecules* **1979**, *12*, 429.
- (21) Perly, B.; Chachaty, C.; Tsutsumi, A. *J. Am. Chem. Soc.* **1980**, *102*, 1521.
- (22) Cole, K. S.; Cole, R. H. *J. Chem. Phys.* **1941**, *9*, 329.
- (23) Connor, T. M. *Trans. Faraday Soc.* **1964**, *60*, 1574.
- (24) Flory, P. J. "Statistical Mechanics of Chain Molecules"; Interscience: New York, 1969.
- (25) Kopple, K. D.; Wiley, G. R.; Tauke, P. *Biopolymers* **1973**, *12*, 627.
- (26) Fischman, A. J.; Wyssbrod, H. R.; Agosta, W. C.; Cowburn, D. *J. Am. Chem. Soc.* **1978**, *100*, 54.
- (27) London, R. E.; Avitabile, J. *J. Am. Chem. Soc.* **1977**, *99*, 7765.
- (28) Tonelli, A. E.; Bovey, F. A. *Macromolecules* **1970**, *3*, 410.
- (29) Levy, G. C.; Axelson, D. E.; Schwarz, R.; Hochmann, J. *J. Am. Chem. Soc.* **1978**, *100*, 410.
- (30) Ghesquiere, D.; Tsutsumi, A.; Chachaty, C. *Macromolecules* **1979**, *12*, 775.
- (31) Woodhouse, D. R.; Derbyshire, W.; Lillford, P. *J. Magn. Reson.* **1975**, *19*, 267.
- (32) Darke, A.; Finer, E. G. *Biopolymers* **1975**, *14*, 441.

## Conformation of *cyclo*(L-Alanylglycyl- $\epsilon$ -aminocaproyl), a Cyclized Dipeptide Model for a $\beta$ Bend. 1. Conformational Energy Calculations<sup>1a</sup>

G. Némethy, J. R. McQuie, M. S. Pottle, and H. A. Scheraga\*<sup>1b</sup>

Baker Laboratory of Chemistry, Cornell University, Ithaca, New York 14853.  
Received August 7, 1980

**ABSTRACT:** The cyclized peptide derivative *cyclo*(L-alanylglycyl- $\epsilon$ -aminocaproyl) contains three peptide groups. These are constrained to form a  $\beta$  bend because the distance between the C <sup>$\alpha$</sup>  and C' atoms of the  $\epsilon$ -aminocaproyl residue cannot exceed 5.04 Å, even when the alkyl chain is fully stretched. Therefore, this molecule serves as a model compound for bends. Its experimentally observed physical properties can be used as standards for the detection of the presence of bends in peptides. An analysis of the complete conformational space of this molecule has been carried out, using energy computation. The conformational space of the L-Ala-Gly dipeptide was mapped in a search for low-energy conformations which permit ring closure with the  $\epsilon$ -aminocaproyl residue. A numerical search method was used to achieve ring closure. Locally stable conformations were found by energy minimization. Low-energy conformations occur only when all three peptide groups are in the trans conformation because the presence of even one cis peptide group raises the energy by at least 9.7 kcal/mol. Ten low-energy conformations of minimum energy were found. Two are type II bends, with relative energies 0.00 and 0.93 kcal/mol. Five are type I and III bends, with relative energies ranging from 0.74 to 1.59 kcal/mol. Three are type I' and III' bends, with relative energies ranging from 2.80 to 3.08 kcal/mol. These results suggest that the molecule exists predominantly as a type II bend, with small amounts of type I and III bend conformations present. This prediction was borne out by experimental measurements in solution and in the solid state (reported in two accompanying papers).

## I. Introduction

Bends constitute one of the important local conformational features of proteins, along with  $\alpha$  helices and extended chains.<sup>2</sup> About 17% of all dipeptide sequences in many proteins of known structure occur as bends or com-

binations of bends.<sup>2,3</sup> The geometrical features of bends have been characterized by Venkatachalam,<sup>4</sup> who described and classified bend conformations into types I, II, and III. A more general classification of bends into several additional types was introduced by Lewis et al.<sup>5</sup> They